RESEARCH   **Open Access**

Identification of key genes and long non-coding RNA expression profiles in osteoporosis with rheumatoid arthritis based on bioinformatics analysis

Jin-yu An[1*], Xing-na Ma[2], Hui-long Wen[1] and Hui-dong Hu[1]

Abstract

Background Although rheumatoid arthritis (RA) is a chronic systemic tissue disease often accompanied by osteoporosis (OP), the molecular mechanisms underlying this association remain unclear. This study aimed to elucidate the pathogenesis of RA and OP by identifying differentially expressed mRNAs (DEmRNAs) and long non-coding RNAs (lncRNAs) using a bioinformatics approach.

Methods Expression profiles of individuals diagnosed with OP and RA were retrieved from the Gene Expression Omnibus database. Differential expression analysis was conducted. Gene ontology (GO) and Kyoto Encyclopedia of Genes and Genomes pathway (KEGG) pathway enrichment analyses were performed to gain insights into the functional categories and molecular/biochemical pathways associated with DEmRNAs. We identified the intersection of common DEmRNAs and lncRNAs and constructed a protein-protein interaction (PPI) network. Correlation analysis between the common DEmRNAs and lncRNAs facilitated the construction of a coding-non-coding network. Lastly, serum peripheral blood mononuclear cells (PBMCs) from patients with RA and OP, as well as healthy controls, were obtained for TRAP staining and qRT-PCR to validate the findings obtained from the online dataset assessments.

Results A total of 28 DEmRNAs and 2 DElncRNAs were identified in individuals with both RA and OP. Chromosomal distribution analysis of the consensus DEmRNAs revealed that chromosome 1 had the highest number of differential expression genes. GO and KEGG analyses indicated that these DEmRNAs were primarily associated with " platelets (PLTs) degranulation", "platelet alpha granules", "platelet activation", "tight junctions" and "leukocyte transendothelial migration", with many genes functionally related to PLTs. In the PPI network, MT-ATP6 and PTGS1 emerged as potential hub genes, with MT-ATP6 originating from mitochondrial DNA. Co-expression analysis identified two key lncRNA-mRNA pairs: $RP11-815J21.2$ with $MT-ATP6$ and $RP11-815J21.2$ with PTGS1. Experimental validation confirmed significant differential expression of RP11-815J21.2, MT-ATP6 and PTGS1 between the healthy controls and the RA + OP groups. Notably, knockdown of RP11-815J21.2 attenuated TNF + IL-6-induced osteoclastogenesis.

*Correspondence:
Jin-yu An
ajy_428@126.com
Full list of author information is available at the end of the article

Conclusions This study successfully identified shared dysregulated genes and potential therapeutic targets in individuals with RA and OP, highlighting their molecular similarities. These findings provide new insights into the pathogenesis of RA and OP and suggest potential avenues for further research and targeted therapies.

Keywords Osteoporosis, Rheumatoid arthritis, lncRNA, Differentially expressed genes, Protein-protein interaction network, Co-expression network

Introduction

Rheumatoid arthritis (RA) is a chronic and progressive autoimmune disease characterized by systemic inflammation, joint destruction, and extra-articular manifestations [1]. RA not only causes local erosions and periarticular bone loss but also triggers early-onset bone loss [2]. Due to inflammation-driven osteoclast activation, RA is considered a significant risk factor for osteoporosis (OP) [3]. Previous study has demonstrated that the prevalence of OP in RA patients is significantly higher [4]. OP, a prevalent skeletal disorder, is characterized by decreased bone density and altered bone structure [5], which increases susceptibility to fractures, including both vertebral and non-vertebral fractures [6]. Osteoporotic fractures can result in persistent pain, significant morbidity and mortality, and increased healthcare expenses [7]. Therefore, effective treatment of OP is crucial to minimize fracture risk in patients with RA.

RA and OP are multifaceted diseases with common pathophysiological mechanisms, particularly concerning bone health [8, 9]. A central feature of both conditions is an imbalance between bone resorption and formation, largely due to excessive osteoclasts activation. Osteoclasts, which break down bone tissue, lead to decreased bone mineral density and increased fractures risk, a hallmark of OP. Osteoclasts are derived from hematopoietic stem cells in the bone marrow [10] and their activation is regulated by various factors, including growth factors and hormones [11]. The receptor activator of nuclear factor-κB ligand (RANKL) and macrophage colony-stimulating factor (M-CSF) are key players in osteoclast differentiation [12]. M-CSF encourages the proliferation and survival of osteoclast precursors, while RANKL is crucial for the differentiation and activation of mature osteoclasts [13]. Inflammatory cytokines such as TNF-α, IL-1, IL-6, and IL-17 have been found to upregulate RANKL expression [14], indicating that at the molecular level, RA and OP share a common feature of altered gene expression. Thus, therapies that inhibit RANKL or inflammatory cytokines can help to balance bone remodeling and reduce bone loss in both conditions [15, 16].

Long non-coding RNAs (lncRNAs), RNA molecules over 200 nucleotides in length, are important epigenetic regulators that control gene expression and influence multiple biological processes [17]. Accumulating evidence suggests that lncRNAs play significant roles in bone remodeling, thus increasing our understanding of the molecular mechanisms underlying OP [17]. LncRNAs can affect bone homeostasis and OP development through various signaling pathways and regulatory networks. In addition, they are hypothesized to play key roles in differentiating and activation of CD4 + T cells [18] and have been reported to function as both inhibitors and promoters of osteogenic differentiation [19], a process important for bone formation. Although these findings suggest that lncRNAs may contribute to the complex mechanisms underlying both RA and OP by influencing immune responses and bone metabolism, further research is needed to fully understand the specific roles and implications of lncRNAs in these conditions.

This study was designed to analyze the expression profiles of mRNAs and lncRNAs with abnormal expression in RA and OP and to explore their potential functions. Additionally, we evaluated the clinical significance of lncRNAs and assessed their potential as diagnostic and prognostic biomarkers, with the goal of identifying novel therapeutic targets related to OP in patients with RA.

Materials and methods

Datasets and data retrieval

The GSE94519 and GSE152293 datasets were retrieved from the Gene Expression Omnibus (GEO) database (http://www.ncbi.nlm.nih.gov/geo/). The microarray dataset GSE94519 consisted of 6 samples, including 3 samples from individuals with RA and 3 control samples. This dataset was generated using the GPL20115 platform. The RNA sequencing dataset GSE152293 included 3 samples from individuals with OP and 3 control samples, performed on the Illumina HiSeq 2000 (GPL11154) platform. Principal component analysis (PCA) was conducted on both datasets to reduce dimensionality and assess data quality control measures.

Screening of differentially expressed mRNAs (DEmRNAs) and long non-coding RNAs (DElncRNAs)

Probes in the GSE94519 data file were annotated using the platform annotation file, and any probes without matching gene symbols were removed. For multiple probes mapping to the same gene, expression values were averaged to obtain the final expression value. The expression levels of mRNAs and lncRNAs were evaluated using the FPKM values obtained from the GSE152293 dataset. The Ensembl database (version 104, http://www.ensembl.org/index.html) [20] and the platform annotation file

were used to identify mRNAs and lncRNAs, respectively. Transcripts not included in the database or the platform file were excluded from the analysis. Differential analysis was performed using the limma package in the R computing environment [21]. DEmRNAs and DElncRNAs were identified based on the criteria of $|\log_2 FC| > 1$ and a p-value < 0.05.

Volcano plots were generated using the gplots package in the R platform to visualize differentially expressed mRNAs and lncRNAs. The venn Diagram package [22] was utilized to determine the overlap of DEmRNAs and DElncRNAs between the datasets.

Functional enrichment analysis

Functional enrichment analysis of DEmRNAs was performed in R using the clusterProfiler package [23]. Gene Ontology (GO) analysis, encompassing molecular functions (MF), biological processes (BP), and cellular components (CC), provided comprehensive information on gene functions. Additionally, KEGG pathway enrichment analysis was performed to identify enriched pathway terms, with a significance threshold of $p < 0.05$.

Circular visualization of the common DEmRNAs

To visualize the common DEmRNAs, including their gene symbols and chromosomal locations, the RCircos package in R [24] was employed. This facilitated a comprehensive and visually informative manner, providing a clearer understanding of the genomic distribution of the identified genes.

Construction of the protein-protein interaction (PPI) network and analysis of hub genes

To analyze the interactions among the proteins encoded by the differentially expressed genes, a PPI network was constructed using the Search Tool for the Retrieval of Interacting Genes (STRING) database [25]. The common DEmRNAs were submitted to the STRING, and interactions with a minimum interaction score of 0.4 were considered. The resulting PPI network was visualized using Cytoscape software [26]. CytoHubba, a plugin app for Cytoscape, was utilized to identify hub genes within the PPI network, providing insights into the central proteins potentially playing crucial roles in the network's overall structure and function.

lncRNA-mRNA co-expression network

To account for batch effects and obtain a consensus set of common DEmRNAs and DElncRNAs between the two datasets, batch correction techniques and data normalization were applied. To ensure the effectiveness of the batch correction, we conducted PCA before and after applying the ComBat correction. PCA plots were generated to visualize the differences and verify that the batch

effects were adequately mitigated. The Pearson correlation coefficient between lncRNA and mRNA expression levels was calculated using the R function cor.test, with a threshold of Pearson correlation coefficient > 0.6 and p-value < 0.05 to identify significant correlations. ased on these criteria, a lncRNA-mRNA network was constructed using Cytoscape, allowing for visual representation and analysis of the interactions between the identified lncRNAs and mRNAs.

Patients, sampling and grouping

Serum samples were collected from patients diagnosed with RA and OP (RA+OP) treated at our hospital from January 2023 to April 2023, and from healthy volunteers (Healthy) during the same period. All clinical samples were collected with the approval of the Ethics Committee of Chanzhou Tumor Hospital (approval number: 2023 (SR) NO.018).

Peripheral blood mononuclear cells (PBMCs) were isolated from the collected blood samples using a density gradient centrifugation method with Ficoll-Paque PLUS (GE Healthcare). The isolated PBMCs were cultured in RPMI-1640 medium (Gibco) supplemented with 10% fetal bovine serum (FBS, Gibco) and 1% penicillin-streptomycin (Gibco) at 37 °C under 5% CO_2.

The Control group consisted of cells cultured under normal conditions without any treatment. The sh-NC group involved cells transfected with negative control shRNA. In the sh-RP11-815J21.2 group, the cells were transfected with *RP11-815J21.2 shRNA*. Additionally, the TNF+IL-6 group was created by treating the cells with TNF (50 ng/mL) and IL-6 (50 ng/mL) for 24 h. To evaluate the impact of shRNA transfection in the presence of TNF and IL-6, the TNF+IL-6+sh-NC group was established, where cells were transfected with negative control shRNA followed by TNF and IL-6 treatment for 24 h. Similarly, the TNF+IL-6+sh-RP11-815J21.2 group was formed by transfecting cells with RP11-815J21.2 shRNA, followed by TNF and IL-6 treatment for 24 h.

shRNA transfection

For shRNA transfection, cells were seeded in 6-well plates at a density of 1×10^6 cells/well and allowed to adhere overnight. Transfections were performed using Lipofectamine 3000 (Invitrogen) according to the manufacturer's protocol. Specifically, 100 nM of either negative control shRNA or RP11-815J21.2 shRNA was used. Transfection efficiency was monitored using a fluorescence microscope and confirmed by qRT-PCR.

Quantitative reverse transcription polymerase chain reaction (qRT-PCR)

To investigate the expression levels of specific genes, qRT-PCR was performed. First, we measured the

expression levels of lncRNA RP11-815J21.2, MT-ATP6 and PTGS1 in the serum samples obtained from both the RA+OP and Healthy groups. Additionally, we determined the expression level of lncRNA RP11-815J21.2 in peripheral blood mononuclear cells (PBMCs) isolated from the RA+OP and Healthy groups, and the expression level of lncRNA RP11-815J21.2 in cells derived from the sh-NC and sh-RP11-815J21.2 experimental groups. The primer sequence used for RP11-815J21.2 is as follows:

GTGGATCTTGTGAGCTGGGTTGCCTTGCTGTG GTGCTTTCGGACTCGCTAACTATGTTATCACACA GTTTTGCAACCAAATCGCCACTAGAAGTCACTGT GTTCTGTTGACATGCAGAGTCTGCACAAAGTTTA TCGTCTCCAGTTGTAGAACAAATGGCTGGAATCA CCACAGAATTCTGATCTACTGGAGCATCAGCACT CTCCTCACGACTTCGTGAAGTTTCCGTTTCTGCT GTTTTTTCAGTGGAGGTTTCTTCATTACTAAATG CAAGTGAAGACTCAGCAGGTTTGTTACCATCCAG GGAACTGGCAGCAGGGGCACAGTTTGGAACACT GATTTTATCCACAGGCTTACTTGTGACGTGCACG TCAGAGGCTCCAGCTGTGCCAATATTAGAGTTCT CAAATCTTTCCTTTGTACTTTCCCCTCCCTGAAG CACATTCTTCCAAACAGTGGCATCTGGGTTCATG AGCCCATGTTCCATTTCCCCTGCAGTGTCTGGGG TACTGACATTTGTTGTTGAAATGCCTCCCAGTTC ACCTCCAGAGGAATACTGGGCTGTGCCTGGCTC CATGACCAAGTCTCTCTGAAGCACAGCATCTCCA CTGCTCAGGGACTCCTGGTCTGTGGGCATTCCA GAAGATTTTGTTCCAGTTTCTTCATTTCTGTTTC CACAGGACGAAAGGCCTTCCGTGCCCTTTACTC CACAATCAGGCAAGCTCTGAAGGCAGCTGTCTT GATCAGATACAGTTCCAGAGTCCACAATAGGTGC TGGCTCCACCTCTTCCCCTTTTCTTTCCACGCCT TTATTTTTCTTCCTACAGGAACGGTCTGTATTCT CCTCCTCAACTATGCTTGACAAATCACAGGGACT TTCAGTCTGTGCAACAGGGCTCCCTGGGCAGCA CTGAGTGCTCTCAGTCTCTTCAGAAGAAGAAAGT CGCTGAGGG.

Tartrate-resistant acid phosphatase (TRAP) staining
TRAP staining was performed to determine osteoclast activity across the different experimental groups, including the Control group, TNF+IL-6 group, TNF+IL-6+sh-NC group and TNF+IL-6+sh-RP11-815J21.2 group. Following the experimental treatments, the culture medium was removed, and cells were gently washed twice with PBS. Cells were then fixed in 4% paraformaldehyde for 10 min at room temperature. After fixation, cells were washed twice with distilled water. The fixed cells were incubated with the TRAP staining solution at 37 °C for 1 h, protected from light. After incubation, the staining solution was removed, and the cells were washed twice with distilled water to stop the reaction. The cells were then air-dried, and TRAP-positive

osteoclasts were identified by their characteristic dark red staining. Quantitative analysis was conducted to determine the number of TRAP-positive osteoclasts present within each experimental group.

Statistical analysis
Data analysis was performed using R software with the indicated packages, and graphs were plotted using GraphPad Prism. All data are expressed as mean±standard deviation. Student's t-test was used to compare two groups, and one-way ANOVA was used for comparison between multiple groups. $P < 0.05$ was used to indicate statistical differences between comparisons.

Results
Principal component analysis verifying the independence of each group
PCA was conducted to assess the distinguishable differences between samples. The results demonstrated a clear distinction between the RA and control samples in the GSE94519 dataset, as well as between the OP samples and the control samples in the GSE152293 dataset. In Fig. 1A, the vertical axis represents the contribution rate of each principal component, while the horizontal axis indicates the number of principal components. The cumulative contribution rates of PCA1 and PCA2 for the two datasets were 61.4% and 62.6%, respectively, indicating that the first two components might be sufficient to distinguish between these two groups, with each group being independent of the other (Fig. 1B).

Differentially expressed mRNAs and lncRNAs in RA and OP
Aberrantly expressed mRNAs and lncRNAs associated with RA and OP were identified based on the $|\log_2 FC| > 1$ and $p < 0.05$ criteria. Volcano plots were used to visualize the DEmRNAs and DElncRNAs (Fig. 2A and B). For RA, a total of 649 DEmRNAs and 313 DElncRNAs were identified, with 385 DEmRNAs and 89 DElncRNAs were upregulated, and the remainder downregulated. For OP, 535 DEmRNAs were identified, including 227 upregulated and 308 downregulated DEmRNAs. Additionally, 33 lncRNAs were differentially expressed, comprising 7 upregulated and 26 downregulated DElncRNAs.

GO and pathway analysis from each disease group
Given the limited functional annotation of most lncRNAs, their specific roles remain largely unknown. Therefore, to gain insights into their potential functions, we aimed to determine potentially significant DEmRNAs. To understand the biological roles of these DEmRNAs in both RA and OP, GO enrichment analysis was performed, encompassing various categories such as BPs, CCs and MFs (Fig. 3A and C). Additionally, KEGG pathway analysis was conducted to explore the enrichment
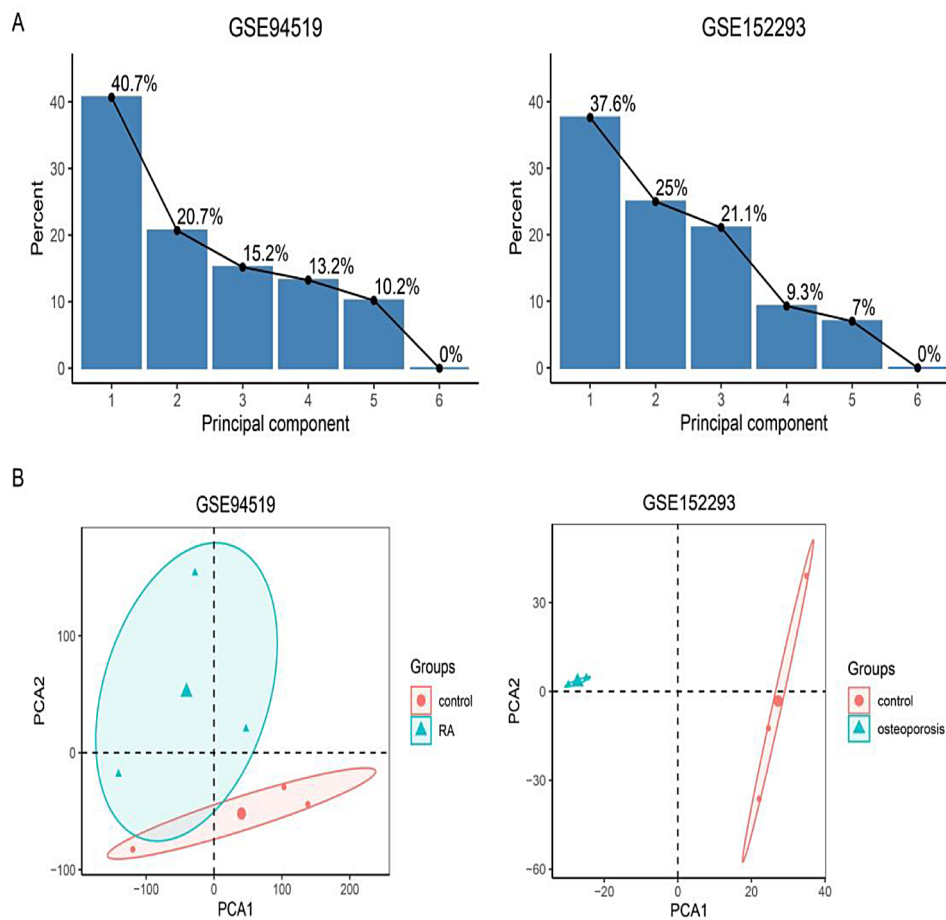
Fig. 1 Results from the principal component analysis (**A**) Bar plots indicated the proportion of variance evaluated for the two datasets. (**B**) Two-dimensional plots with the top two principal components. Horizontal and vertical axes represented the distribution of each sample with PCA1 and PCA2

of signaling pathways associated with the DEmRNAs (Fig. 3B and D). The results indicated that certain DEm-RNAs were commonly enriched in GO terms related to platelet degranulation (BP) and platelet alpha granule (CC), as summarized in Table 1. Furthermore, the KEGG pathway analysis revealed the involvement of several DEmRNAs in pathways related to platelet activation, tight junctions and leukocyte transendothelial migration (Table 2). Notably, significant enrichment was observed for platelet activation, suggesting a prominent association between RA and OP.

Common DEmRNAs and DElncRNAs both in RA and OP
Here, we comprehensively analyzed the DEmRNAs and DElncRNAs in RA and OP. Among the DEmRNAs, a total of 28 mRNAs exhibited differential expression in both diseases. Specifically, 23 mRNAs were upregulated, and 5 mRNAs were downregulated. Additionally, two common lncRNAs, RP11-815J21.2 and CTD-3092A11.2, were identified in both datasets. The Venn diagram (Fig. 4A) visually represents the overlap between the differentially expressed mRNAs and lncRNAs.

Furthermore, a heatmap (Fig. 4B) was generated to illustrate the differences in the expression patterns of the common DEmRNAs, providing a clear overview of the variations in gene expression levels across the samples. Then, chromosome mapping of the consensus DEmRNAs (Fig. 4C) was performed to show the distribution of these genes on different chromosomes, with chromosome 1 containing the highest number of DEGs. Additionally, while differences were observed in the expression of two genes on the X chromosome, no genes were affected on the Y chromosome.

PPI network of common DEmRNAs and hub genes identification
The STRING database was used to investigate the PPI among the common DEmRNAs. Using a predefined criterion of an interaction score > 0.4, 17 DEmRNAs (of the 28 common DEmRNAs) were identified in the PPI network, consisting of 37 nodes and 95 edges, highlighting the connections between these proteins (Fig. 5A). Then, the CytoHubba plugin was used to identify key genes within the PPI network. Using the Maximal Clique
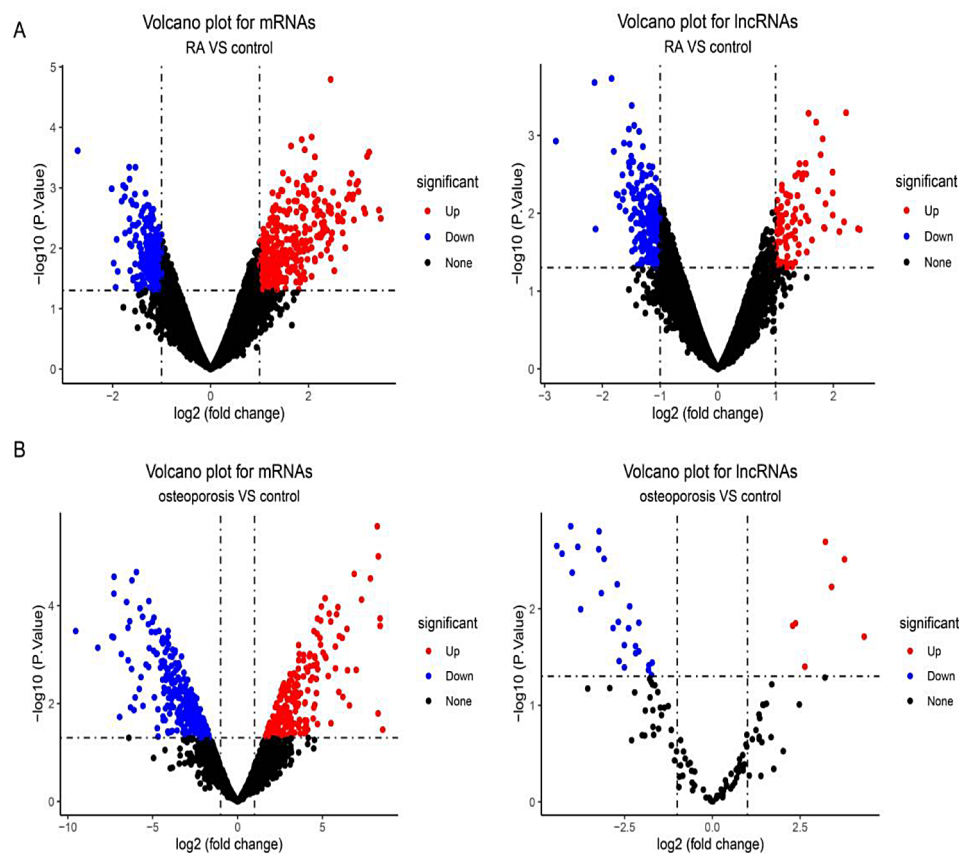
Fig. 2 Volcano plots for mRNAs and lncRNAs in RA and OP. (**A**) Volcano plots showing differentially expressed mRNAs (left) and lncRNAs (right) in RA patients vs. controls. (**B**) Volcano plots showing differentially expressed mRNAs (left) and lncRNAs (right) in OP patients vs. controls. Red dots indicate significantly up-regulated genes (FC > 1, $p < 0.05$), blue dots indicate significantly down-regulated genes (FC < -1, $p < 0.05$), and black dots indicate non-significant genes. RA, Rheumatoid arthritis; OP, Osteoporosis

Centrality (MCC) method, the top 12 key genes were selected (Fig. 5B). Among them, MT-ATP6 and PTGS1 were identified as potential hub genes that might play crucial roles in both RA and OP. Their central positions within the PPI network suggest their significance in RA and OP.

lncRNA-mRNA co-expression network analysis
A co-expression network was constructed to investigate the potential interactions between common lncRNAs and mRNAs based on correlation analysis. LncRNA-mRNA pairs were predicted using criteria of a p-value < 0.05 and a correlation coefficient > 0.6. Functional prediction of lncRNAs was performed based on their co-expressed mRNAs, aiding in identifying candidate biomarkers. The resulting co-expression network (Fig. 6A) consisted of 23 nodes, representing 21 DEmRNAs and 2 DElncRNAs. The network included 1 negative interaction and 22 positive interactions.

Further examination focused on the expression levels of two specific lncRNA-mRNA pairs, RP11-815J21.2-MT-ATP6 and RP11-815J21.2-PTGS1, in both the RA

and OP datasets (Fig. 6B). These pairs exhibited upregulation in both diseases. Notably, MT-ATP6 and PTGS1, the corresponding mRNAs, were predicted to be essential in the PPI network. Additionally, RP11-815J21.2 appeared to regulate the expression of these mRNAs. These findings shed light on the potential regulatory role of RP11-815J21.2 and highlight its relevance in the context of RA and OP.

Next, in light of these results mentioned above, we aimed to provide experimental evidence and functional characterization to support and validate the findings obtained from the initial analysis of online databases.

Differential expression of RP11-815J21.2, MT-ATP6 and PTGS1
To further validate the findings from the initial bioinformatics analysis, we examined the differential expression of RP11-815J21.2, MT-ATP6, and PTGS1 between the Healthy group and the RA+OP group. Compared with the Healthy group, we observed a significant upregulation of RP11-815J21.2, MT-ATP6 and PTGS1 in the serum (Fig. 7A-C) and a significant increase in RP11-815J21.2
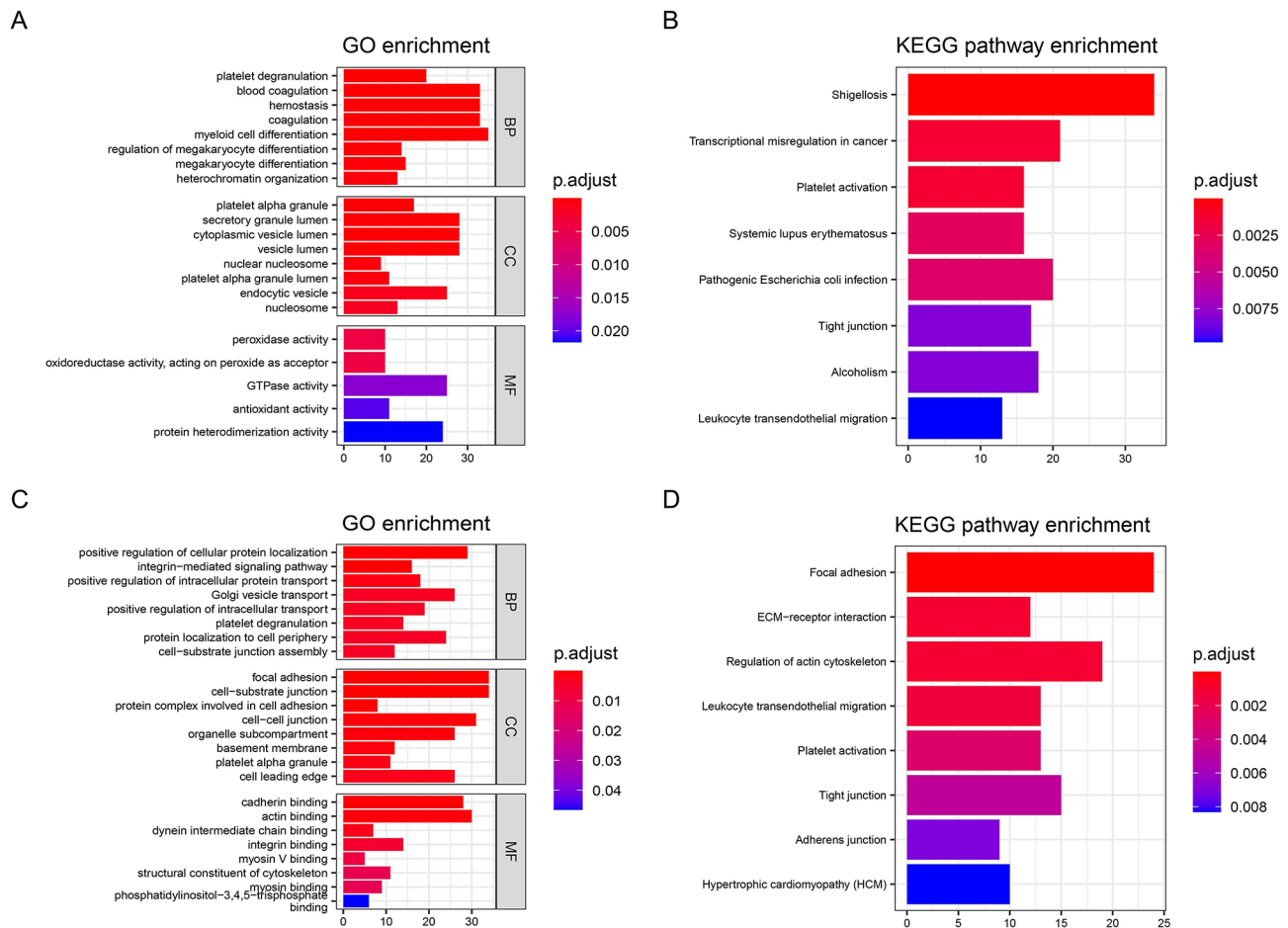
Fig. 3 GO and KEGG pathway enrichment analysis for differentially expressed genes (DEGs) in rheumatoid arthritis (RA) and osteoporosis (OP). (**A**) GO enrichment analysis for DEGs in RA patients vs. controls. (**B**) KEGG pathway enrichment analysis for DEGs in RA patients vs. controls. (**C**) GO enrichment analysis for DEGs in OP patients vs. controls. (**D**) KEGG pathway enrichment analysis for DEGs in OP patients vs. controls. The x-axis shows the number of genes, and the y-axis lists the enriched GO terms or KEGG pathways. The color gradient represents the adjusted *p*-value (*p*.adjust), indicating the significance of the enrichment. GO = Gene Ontology, CC = Cellular Component, MF = Molecular Function, BP = Biological Process, KEGG = Kyoto Encyclopedia of Genes and Genomes

Table 1 Common GO terms between RA and OP

GO term and function	Differentially expressed mRNAs	
	RA	**OP**
GO:0002576-platelet degranulation	PF4,PPBP, F13A1,LY6G6F, GTPBP2,CLU, LYN, TLN1,SRGN, VCL, FERMT3,CTSW, CD9,ABCC4,VTI1B, ALDOA, ITGB3,RAB27B, TMSB4X, TIMP1	TMSB4X, PPBP, TLN1,ACTN1,TGFB1,SPARC, FCER1G, APP, RAB27B, ACTN4,TMX3,ITGA2B, CYB5R1,QSOX1,
GO:0031091-platelet alpha granule	PF4,PPBP, SNCA, F13A1,LY6G6F, TREML1,GTPBP2,CLU, SRGN, FERMT3,CD9,VTI1B, ALDOA, ITGB3,TMSB4X, TIMP1,VAMP7	TMSB4X, PPBP, ACTN1,TGFB1,SPARC, APP, ACTN4 TMX3,ITGA2B, CYB5R1,QSOX1

RA: Rheumatoid arthritis, GO: Gene ontology

in the PBMC cells (Fig. 7D) of the RA + OP group. Conversely, we observed a significant downregulation of RP11-815J21.2 in cells from the sh-RP11-815J21.2 group compared to the sh-NC group (Fig. 7E). These results suggested that these genes might play a role in the pathogenesis of RA and OP.

TRAP-positive osteoclasts in various treatment groups

TRAP-positive osteoclasts, indicative of bone resorption, serve as a marker for osteoclast activity. An increased number of TRAP-positive osteoclasts suggests enhanced osteoclast activity, which contributes to bone loss and OP. Here, we evaluated the effects of different treatments on osteoclastogenesis, specifically in regard to TNF + IL-6 stimulation and RP11-815J21.2 knockdown. TRAP staining results revealed a significant increase in the number of TRAP-positive osteoclasts in the TNF + IL-6 group, TNF + IL-6 + sh-NC

Table 2 Common KEGG pathways between RA and OP

| KEGG ID and pathways | Differentially expressed mRNAs | |
	RA	OP
hsa04611-platelet activation	FCGR2A, AKT3,ACTB, LYN, TLN1,PTGS1,ITGB1,FERMT3,GP1BA, ITGB3,GNA13,MYL12A, MYL12B, GNAS, GP1BB, MAPK1	TLN1,MYL12A, PTGS1,FCER1G, SNAP23,STIM1,APBB1IP, AKT3,ROCK2,ROCK1,PTGIR, ITGA2B, ACTG1
hsa04530-tight junction	CDC42,CLDN22,RAPGEF6,ACTB, CLDN4,CLDN15,ITGB1,AM OTL1,TUBA1B, TUBA1C, MYL6,CLDN10,MYL12A, MYL12B, MAP2K7,MYL9,TUBA8	MYH9,MYL12A, ACTN1,SYNPO, ACTR2,JA M3,ROCK2,ACTN4,TJP2,RO CK1,PRKAB2,DLG3,MYH7B, JAM2,ACTG1
hsa04670-leukocyte transendothelial migration	CDC42,MYL5,CLDN22,CTNNA1,ACTB, CLDN4,CLDN15,ITGB1,VCL, CLDN10,MYL12A, MYL12B, MYL9	MYL12A, ACTN1,PRKCB, ITGAM, JAM3,ROCK2,ACTN4,P TPN11,VAV3,ITGA4,ROCK1,JA M2,ACTG1

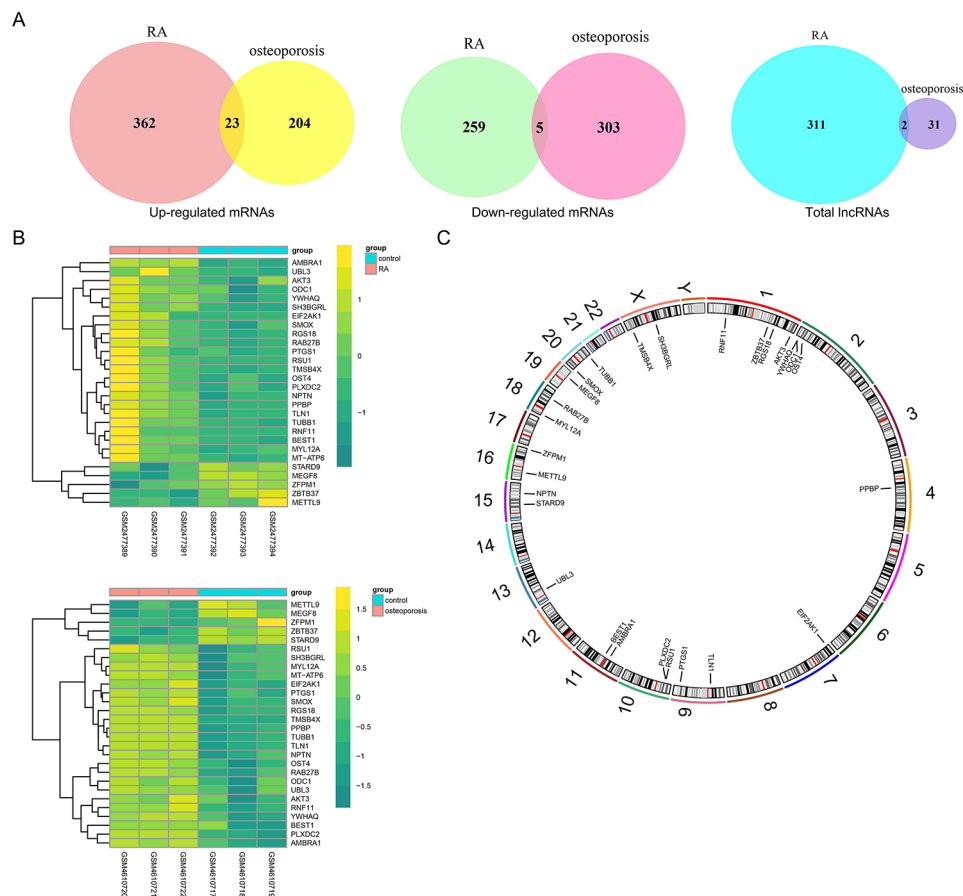RA: Rheumatoid arthritis, KEGG: The Kyoto Encyclopedia of Genes and Genomes

Fig. 4 Analysis of common DEmRNAs and DElncRNAs in rheumatoid arthritis (RA) and osteoporosis (OP). (**A**) Venn diagram demonstrated the intersections of DEmRNAs and DElncRNAs between RA and OP. (**B**) Heat map of common DEmRNAs, with samples grouped by RA and OP. (**C**) Chromosome mapping of consensus DEmRNAs

group and TNF+IL-6+sh-RP11-815J21.2 group, compared to the Control group. Additionally, we observed a significant decrease in the number of TRAP-positive osteoclasts in the TNF+IL-6+sh-RP11-815J21.2 group compared to the TNF+IL-6+sh-NC group, while there was no statistically significant difference in the number

of osteoclasts between the TNF+IL-6 group and the TNF+IL-6+sh-NC group (Fig. 8). These findings suggested that TNF+IL-6 stimulation promoted osteoclastogenesis, and knockdown of RP11-815J21.2 might attenuate this effect.
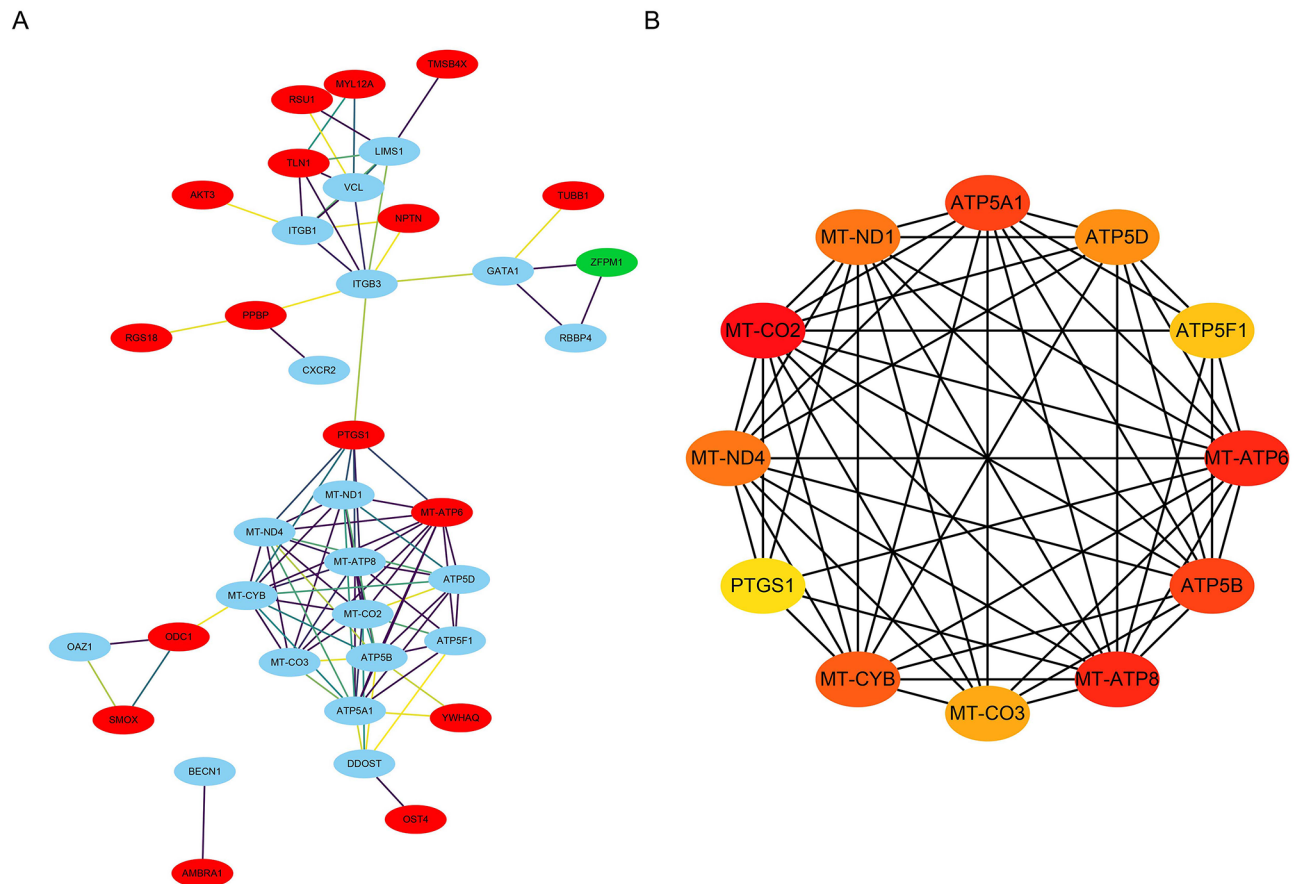
Fig. 5 Protein-protein interaction (PPI) network. (**A**) Using STRING, a total of 17 common DEmRNAs (16 up-regulated genes shown in red and one down-regulated genes shown in green) were filtered into a PPI network. A darker colored line between two proteins indicated a greater interaction. (**B**) The hub genes network: the top 12 genes derived from the MMC method were selected with Cytohubba plugin. Higher ranking is indicated by a redder color

Discussion

The present study investigated the molecular characteristics and potential mechanisms underlying the association between RA and OP through comprehensive analysis of online databases and subsequent experimental validation. Our investigation revealed several key findings, providing insights into the shared pathways and potential biomarkers associated with both diseases.

PCA analysis demonstrated a clear distinction between the RA and control samples in the GSE94519 dataset and between the OP and control samples in the GSE152293 dataset, indicating distinct molecular profiles associated with each condition. This analysis not only validated the initial grouping of samples but also suggested potential molecular signatures that differentiate RA and OP from healthy controls. In addition, we identified a total of 385 upregulated and 264 downregulated DEmRNAs between RA and control samples. Similarly, between OP and control samples, we identified 535 DEmRNAs, including 227 upregulated and 308 downregulated genes. Considering that co-expressed genes often have similar expression patterns and participate in similar BPs [27], we

conducted GO and pathway enrichment analyses. The results revealed that the DEmRNAs in both RA and OP were commonly involved in processes such as "platelet degranulation", "platelet alpha granule", "platelet activation", "tight junction" and "leukocyte transendothelial migration". Most of these genes were found to be associated with platelets.

It has been reported that platelets and platelet-derived microparticles play a role in the inflammatory processes associated with RA [28]. Activated platelets release various cytokines, chemokines and growth factors stored in their α-granules and dense granules, which recruit inflammatory cells to affected tissues and trigger inflammation [29, 30]. These factors may also affect both bone formation and resorption [31]. Several studies have highlighted the supportive effect of PLTs on bone formation, attributed to platelet-derived growth factors (PDGFs) that promote cell proliferation, chemotaxis, differentiation and extracellular matrix synthesis, thereby favoring bone formation [32]. PLTs possess vitamin D receptors, which are less expressed in OP patients and associated with variations in bone mineral density (BMD) [33]. The
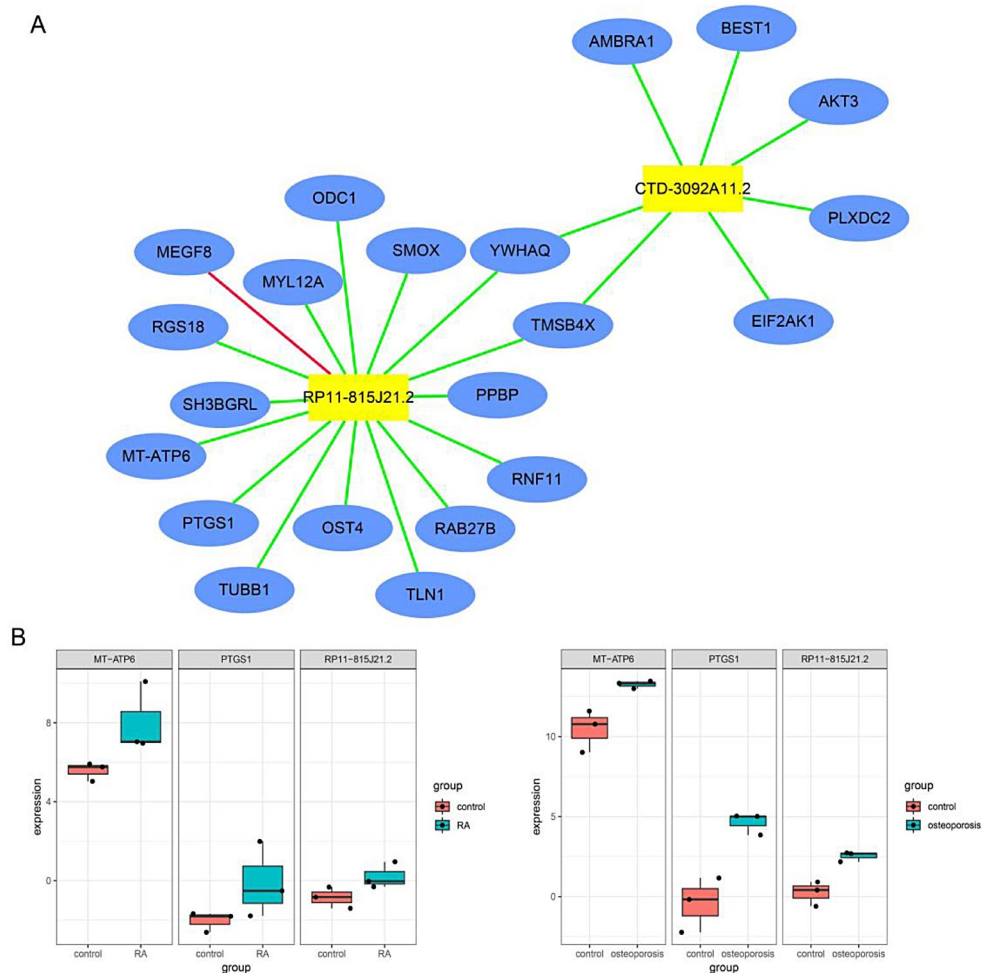
Fig. 6 Co-expression network between common DEmRNAs and DElncRNAs. (**A**) Co-expression network showed the interaction between mRNAs and DElncRNAs Blue ellipse nodes represented mRNAs, yellow square nodes represented DElncRNAs. The red line between mRNAs and lncRNAs indicated a negative correlation, while the green lines indicated a positive correlation. (**B**) Box plot showed the expression pattern of two lncRNA-mRNA pairs (RP11-815J21.2-MTATP6 and RP11-815J21.2-PTGS1)

PLT/lymphocyte ratio has also been correlated with low BMD [34]. Mediators released from PLTs are thought to participate in bone remodeling processes. For instance, epidermal growth factor (EGF) and RANKL cooperatively stimulate osteoclasts, transforming growth factor-beta (TGF-B) enhances osteoprotegerin synthesis, potentially, and thromboxane A2 (TXA2) induces osteoclastogenesis and enhances bone resorption [32, 35]. Chronic inflammation plays a pivotal role in OP, and activated platelets have been implicated in this process [36]. Pro-inflammatory cytokines increase oxidative stress, leading to platelet activation, promoting osteoclast formation, and stimulating bone resorption. Activated PLTs can also impact osteoclastogenesis through prostaglandin and RANKL signaling pathways [37]. Thus, further investigations focusing on platelet-related mechanisms, such as platelet-derived factors or platelet interactions with immune cells and bone cells, could provide deeper insights into the interplay between RA and OP.

To identify common genes shared between RA and OP, we intersected the DEmRNAs from both conditions. A total of 28 common DEmRNAs were identified, including 23 upregulated and 5 downregulated genes. A heatmap provided further evidence of the differential expression of these mRNAs. Additionally, we conducted chromosome mapping analysis to visualize the distribution of these genes across chromosomes. Previous studies have indicated the involvement of X-chromosome genes in autoimmunity, RA, and OP, such as CD99, IRAK-1, LAMP-2, CD40L, TLR7, DDX3X, XIAP, and USP27X [38]. Van Dijk FS et al. found that mutation in PLS3 might result in X-linked OP [39]. Our findings suggest that dysregulated genes on the X-chromosome, specifically SH3BGRL and TMSB4X, may be implicated in the pathogenesis of RA and OP. Additionally, genes on chromosomes 1 and 13
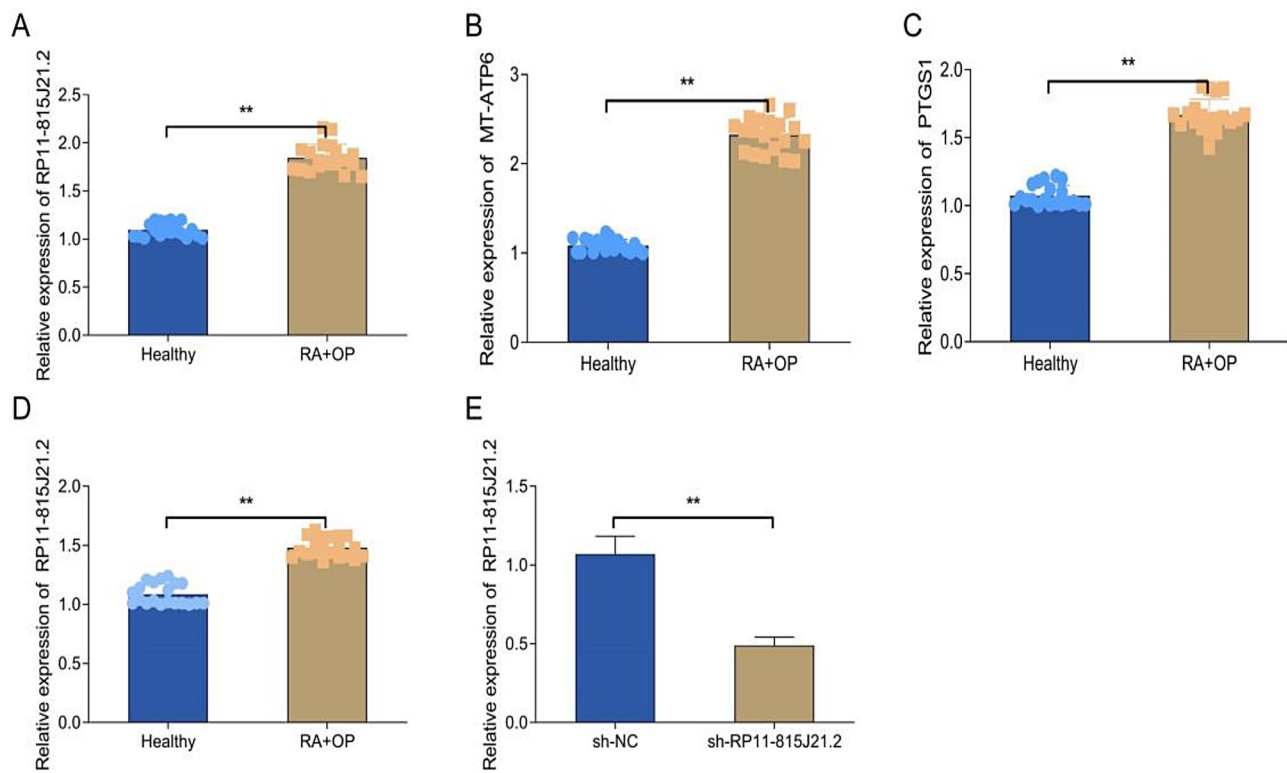
Fig. 7 Differential expression of RP11-815J21.2, MT-ATP6 and PTGS1. (**A**-**C**) Levels of RP11-815J21.2, MT-ATP6 and PTGS1 in the serum of healthy group and RA+OP group. (**D**) Levels of RP11-815J21.2 in PBMC cells of healthy group and RA+OP group. (**E**) Levels of RP11-815J21.2 in sh-NC group and sh-RP11-815J21.2 group. **$p < 0.01$
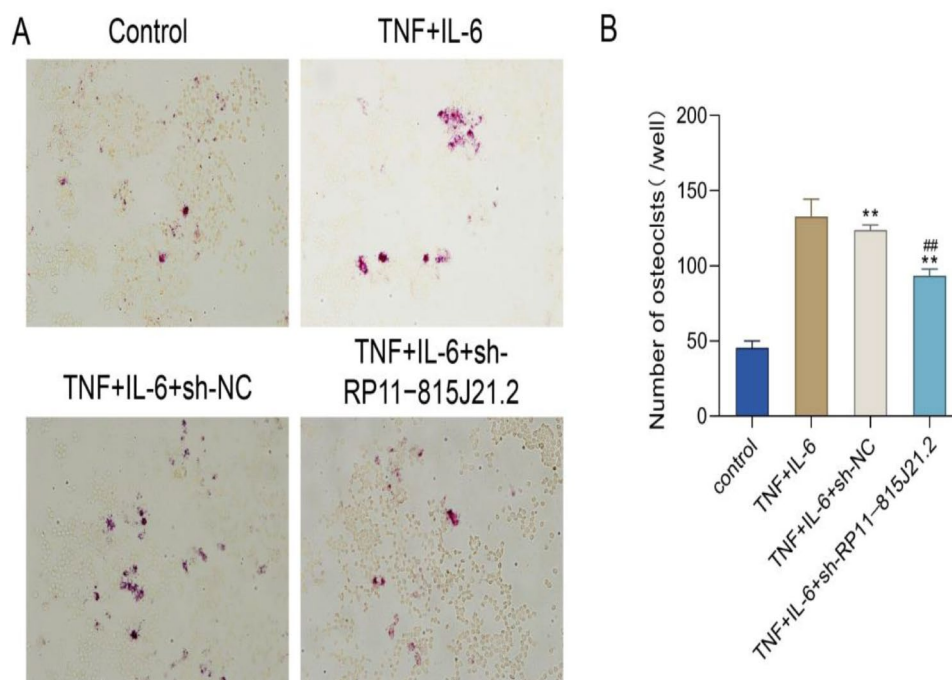

Fig. 8 TRAP staining results. (**A**) TRAP staining in different groups (Magnification: 200 ×). (**B**) Number of osteoclasts in different groups. **$p < 0.01$, compared with the TNF+IL-6 group; ##$p < 0.01$, compared with the TNF+IL-6+sh-NC group

have been implicated in RA and OP [40–42]. Notably, we observed that chromosome 1 contained the highest number of dysregulated genes in our study. The identification of chromosome distribution patterns and the absence of gene expression changes on the Y chromosome provide additional clues for exploring the sex-specific aspects of RA and OP. Future studies can delve into the functional characterization of the common differentially expressed genes and investigate their interactions with other known regulators to gain insights into their roles in disease progression.

The subsequent construction of the PPI network using the common DEmRNAs identified 17 genes as potential key players involved in RA and OP. We identified MT-ATP6 and PTGS1 as hub genes as they were found to play central roles in the molecular network associated with both diseases. These genes could serve as potential therapeutic targets or diagnostic markers. PTGS1 has been associated with various pathological disorders, including inflammation, arthritis, and cancer [43]. The upregulation of PTGS1 and the PTGS2 pathways, involved in arachidonic acid metabolism, have been implicated in the development of rheumatic diseases [44]. Additionally, PTGS1 has been shown to control the osteogenesis of adipose-derived stem cells, suggesting its involvement in osteogenic differentiation [45]. Cho HW et al. reported that PTGS1 was associated with OP [43]. In our study, PTGS1 was found to be overexpressed and enriched in the platelet activation pathway in both RA and OP, indicating its potential role in the pathogenesis of these conditions.

MT-ATP6, the other promising hub gene, is known to derive from mitochondrial DNA. Previous studies have confirmed that each mitochondrion contains multiple copies of mitochondrial DNA (mtDNA), which encode 13 electron transport chain protein subunits and 22 tRNAs and 2rRNAs [46]. Higher levels of mtDNA have been observed in the plasma and synovial fluid of RA patients compared to control subjects. Moreover, mtDNA has been shown to induce the expression of TNF-α through NF-κB activation, contributing to inflammation and tissue injury [47]. Juping Du et al. detected the enrichment of variants in MT-ATP6 in RA patients [48]. In our study, MT-ATP6 was enriched in both RA and OP patients. Interestingly, another mitochondrial DNA mutation, A3243G, in blood leukocytes has been significantly associated with lower bone mineral density [49]. Further evidence supporting mitochondrial dysfunction as a potential contributor to OP comes from studies in mice with a specific knockout of mitochondrial transcription factor A (TFAM) in osteoclasts [50]. Collectively, these findings suggest that accumulated mtDNA mutations may play a significant role in the pathogenesis of RA and OP.

In recent years, the study of lncRNAs has gained significant attention across various fields. However, our understanding of lncRNAs is still in its early stages, and most of them remain largely unexplored. The construction of a co-expression network between common lncRNAs and mRNAs revealed potential regulatory relationships and highlighted the significance of RP11-815J21.2 in the context of RA and OP. Notably, we discovered two potential key pairs of lncRNAs and target mRNAs, namely RP11−815J21.2-MT−ATP6 and RP11−815J21.2-PTGS1. Previous studies have demonstrated the relevance of MT−ATP6 and PTGS1 to RA and OP, and our findings showed significantly higher expression of these pairs compared to the control group. However, to the best of our knowledge, no previous reports have investigated the role of the novel lncRNA RP11−815J21.2 in any disease, and there is no direct evidence to suggest that RP11-815J21.2 can regulate MT-ATP6 currently. Thus, we performed experimental validation to verify the findings obtained from the initial analyses. The up-regulation of RP11-815J21.2, MT-ATP6 and PTGS1 in the serum and PBMC cells of the RA+OP group indicated their potential as biomarkers for detecting and monitoring these conditions. Furthermore, these genes represent potential therapeutic targets for developing precision therapies. By understanding the specific molecular profiles associated with each patient, personalized treatment strategies can be tailored to target the dysregulated pathways. Additionally, the differential expression of these genes provides molecular evidence linking RA and OP, allowing for an integrated approach to managing the comorbidity of these diseases. Notably, the current study has not been able to directly demonstrate an interaction between RP11-815J21.2 and MT-ATP6. Therefore, future studies should consider employing techniques such as dual luciferase reporter gene assays or RNA pull-down assays to confirm the direct regulatory relationships.

Overall, these findings have the potential to contribute to improved diagnostic accuracy, targeted therapies, and personalized treatment plans, ultimately enhancing patient outcomes and quality of life.

Conclusion

In conclusion, our study revealed co-differentially expressed mRNAs and lncRNAs in RA and OP and provided insights into the shared pathways and potential biomarkers associated with both diseases. Platelet-related mechanisms, such as platelet-derived factors and their interactions with immune cells and bone cells, were highlighted as important factors in the pathogenesis of RA and OP. The identification of hub genes MT-ATP6 and PTGS1, along with the novel lncRNA RP11-815J21.2, expands our understanding of the molecular mechanisms underlying these diseases. Further research is needed to

validate the clinical utility and functional significance of these findings in larger patient cohorts and to explore their potential as targets for therapeutic intervention.

Abbreviations

GEO	Gene Expression Omnibus
PCA	Principal component analysis
GO	Gene Ontology
KEGG	Kyoto Encyclopedia of Genes
MF	Molecular functions
BP	Biological processes
CC	Cellular components
PDGF	Platelet-Derived Growth Factor
BMD	Bone mineral density
EGF	Epidermal Growth Factor
STING	Stimulator of Interferon Genes
PPI	Protein-Protein Interaction
RNAKL	Receptor Activator of Nuclear Factor-κ B Ligand
TGF	Transforming growth factor
TXA2	Thromboxane A2

Declarations

Ethics approval and consent to participate
This study was approved by the Research and Ethical Review Board of the Chanzhou Tumor Hospital (approval No: 2023 (SR) NO.018), and written informed consent was obtained from all participants.

Consent for publication
Not applicable.

Competing interests
The authors declare no competing interests.

Author details
¹Department of Orthopedics, Changzhou Fourth People's Hospital, Changzhou 213000, China
²Department of Pediatric, Changzhou Fourth People's Hospital, Changzhou 213000, China

References
1. Laki J, Lundstrom E, Snir O, Ronnelid J, Ganji I, Catrina AI, Bengtsson C, Saevarsdottir S, Wick MC, Alfredsson L, et al. Very high levels of anti-citrullinated protein antibodies are associated with HLA-DRB1*15 non-shared epitope allele in patients with rheumatoid arthritis. Arthritis Rheum. 2012;64(7):2078–84.
2. Smolen JS, Aletaha D, McInnes IB. Rheumatoid arthritis. Lancet. 2016;388(10055):2023–38.
3. Park JH, Park EK, Koo DW, Lee S, Lee SH, Kim GT, Lee SG. Compliance and persistence with oral bisphosphonates for the treatment of osteoporosis in female patients with rheumatoid arthritis. BMC Musculoskelet Disord. 2017;18(1):152.
4. Moshayedi S, Tasorian B, Almasi-Hashiani A. The prevalence of osteoporosis in rheumatoid arthritis patient: a systematic review and meta-analysis. Sci Rep. 2022;12(1):15844.
5. Wegierska M, Dura M, Blumfield E, Zuchowski P, Waszczak M, Jeka S. Osteoporosis diagnostics in patients with rheumatoid arthritis. Reumatologia. 2016;54(1):29–34.
6. Kim SY, Schneeweiss S, Liu J, Daniel GW, Chang CL, Garneau K, Solomon DH. Risk of osteoporotic fracture in a large population-based cohort of patients with rheumatoid arthritis. Arthritis Res Ther. 2010;12(4):R154.
7. Papaioannou A, Kennedy CC, Ioannidis G, Sawka A, Hopman WM, Pickard L, Brown JP, Josse RG, Kaiser S, Anastassiades T, et al. The impact of incident fractures on health-related quality of life: 5 years of data from the Canadian Multicentre osteoporosis study. Osteoporos Int. 2009;20(5):703–14.
8. Raterman HG, Bultink IE, Lems WF. Osteoporosis in patients with rheumatoid arthritis: an update in epidemiology, pathogenesis, and fracture prevention. Expert Opin Pharmacother. 2020;21(14):1725–37.
9. Chen R, Huang Q, Chen L. Development and Validation of Machine Learning models for Prediction of Fracture Risk in patients with Elderly-Onset Rheumatoid Arthritis. Int J Gen Med. 2022;15:7817–29.
10. Bar-Shavit Z. The osteoclast: a multinucleated, hematopoietic-origin, bone-resorbing osteoimmune cell. J Cell Biochem. 2007;102(5):1130–9.
11. Rodan GA, Martin TJ. Therapeutic approaches to bone diseases. Science. 2000;289(5484):1508–14.
12. Jang HY, Lee HS, Noh EM, Kim JM, You YO, Lee G, Koo JH, Lim H, Ko S, Kim JS, et al. Aqueous extract of Chrysanthemum morifolium Ramat. Inhibits RANKL-induced osteoclast differentiation by suppressing the c-fos/NFATc1 pathway. Arch Oral Biol. 2021;122:105029.
13. Feng X, Teitelbaum SL. Osteoclasts: New insights. Bone Res. 2013;1(1):11–26.
14. Maruotti N, Corrado A, Cantatore FP. Osteoporosis and rheumatic diseases. Reumatismo. 2014;66(2):125–35.
15. Naidu VG, Dinesh Babu KR, Thwin MM, Satish RL, Kumar PV, Gopalakrishna-kone P. RANKL targeted peptides inhibit osteoclastogenesis and attenuate adjuvant induced arthritis by inhibiting NF-kappaB activation and down regulating inflammatory cytokines. Chem Biol Interact. 2013;203(2):467–79.
16. Yao Z, Lei W, Duan R, Li Y, Luo L, Boyce BF. RANKL cytokine enhances TNF-induced osteoclastogenesis independently of TNF receptor associated factor (TRAF) 6 by degrading TRAF3 in osteoclast precursors. J Biol Chem. 2017;292(24):10169–79.
17. Mattick JS, Amaral PP, Carninci P, Carpenter S, Chang HY, Chen LL, Chen R, Dean C, Dinger ME, Fitzgerald KA, et al. Long non-coding RNAs: definitions, functions, challenges and recommendations. Nat Rev Mol Cell Biol. 2023;24(6):430–47.
18. Li M, Ma K, Feng Z, Wang J, Zhou X, Zhou L. Differential long non-coding RNA expression profiles in the peripheral blood and CD4(+) T cells of patients with active rheumatoid arthritis. Exp Ther Med. 2020;20(1):461–71.
19. Teng Z, Zhu Y, Zhang X, Teng Y, Lu S. Osteoporosis is characterized by altered expression of Exosomal Long non-coding RNAs. Front Genet. 2020;11:566959.
20. Aken BL, Ayling S, Barrell D, Clarke L, Curwen V, Fairley S, Fernandez Banet J, Billis K, Garcia Giron C, Hourlier T et al. The Ensembl gene annotation system. *Database (Oxford)* 2016, 2016.
21. Ritchie ME, Phipson B, Wu D, Hu Y, Law CW, Shi W, Smyth GK. Limma powers differential expression analyses for RNA-sequencing and microarray studies. Nucleic Acids Res. 2015;43(7):e47.
22. Chen H, Boutros PC. VennDiagram: a package for the generation of highly-customizable Venn and Euler diagrams in R. BMC Bioinformatics. 2011;12:35.
23. Yu G, Wang LG, Han Y, He QY. clusterProfiler: an R package for comparing biological themes among gene clusters. OMICS. 2012;16(5):284–7.
24. Zhang H, Meltzer P, Davis S. RCircos: an R package for Circos 2D track plots. BMC Bioinformatics. 2013;14:244.
25. Szklarczyk D, Gable AL, Nastou KC, Lyon D, Kirsch R, Pyysalo S, Doncheva NT, Legeay M, Fang T, Bork P, et al. The STRING database in 2021: customizable protein-protein networks, and functional characterization of user-uploaded gene/measurement sets. Nucleic Acids Res. 2021;49(D1):D605–12.
26. Doncheva NT, Morris JH, Gorodkin J, Jensen LJ. Cytoscape StringApp: Network Analysis and Visualization of Proteomics Data. J Proteome Res. 2019;18(2):623–32.

27. Zhu N, Hou J, Wu Y, Li G, Liu J, Ma G, Chen B, Song Y. Identification of key genes in rheumatoid arthritis and osteoarthritis based on bioinformatics analysis. Med (Baltim). 2018;97(22):e10997.

28. Boilard E, Nigrovic PA, Larabee K, Watts GF, Coblyn JS, Weinblatt ME, Massarotti EM, Remold-O'Donnell E, Farndale RW, Ware J, et al. Platelets amplify inflammation in arthritis via collagen-dependent microparticle production. Science. 2010;327(5965):580–3.

29. Cafaro G, Bartoloni E, Alunno A, Gerli R. Platelets: a potential target for rheumatoid arthritis treatment? Expert Rev Clin Immunol. 2019;15(1):1–3.

30. Flad HD, Brandt E. Platelet-derived chemokines: pathophysiology and therapeutic aspects. Cell Mol Life Sci. 2010;67(14):2363–86.

31. Ciovacco WA, Cheng YH, Horowitz MC, Kacena MA. Immature and mature megakaryocytes enhance osteoblast proliferation and inhibit osteoclast formation. J Cell Biochem. 2010;109(4):774–81.

32. Khan FA, Parayaruthottam P, Roshan G, Menon V, Fidha M, Fernandes AK. Platelets and their pathways in Dentistry: systematic review. J Int Soc Prev Community Dent. 2017;7(Suppl 2):S55–60.

33. Akbal A, Gokmen F, Gencer M, Inceer BS, Komurcu E. Mean platelet volume and platelet distribution width can be related to bone mineralization. Osteoporos Int. 2014;25(9):2291–5.

34. Eroglu S, Karatas G. Platelet/lymphocyte ratio is an independent predictor for osteoporosis. Saudi Med J. 2019;40(4):360–6.

35. Li XS, Zhang JR, Meng SY, Li Y, Wang RT. Mean platelet volume is negatively associated with bone mineral density in postmenopausal women. J Bone Min Metab. 2012;30(6):660–5.

36. Gawaz M, Langer H, May AE. Platelets in inflammation and atherogenesis. J Clin Invest. 2005;115(12):3378–84.

37. Sharif PS, Abdollahi M. The role of platelets in bone remodeling. Inflamm Allergy Drug Targets. 2010;9(5):393–9.

38. Barik RR, Bhatt LK. Emerging epigenetic targets in rheumatoid arthritis. Rheumatol Int. 2021;41(12):2047–67.

39. van Dijk FS, Zillikens MC, Micha D, Riessland M, Marcelis CL, de Die-Smulders CE, Milbradt J, Franken AA, Harsevoort AJ, Lichtenbelt KD, et al. PLS3 mutations in X-linked osteoporosis with fractures. N Engl J Med. 2013;369(16):1529–36.

40. Lopez Herraez D, Martinez-Bueno M, Riba L, Garcia de la Torre I, Sacnun M, Goni M, Berbotto GA, Paira S, Musuruana JL, Graf CE, et al. Rheumatoid arthritis in Latin americans enriched for amerindian ancestry is associated with loci in chromosomes 1, 12, and 13, and the HLA class II region. Arthritis Rheum. 2013;65(6):1457–67.

41. Chen XF, Zhu DL, Yang M, Hu WX, Duan YY, Lu BJ, Rong Y, Dong SS, Hao RH, Chen JB, et al. An osteoporosis risk SNP at 1p36.12 acts as an allele-specific enhancer to modulate LINC00339 expression via Long-Range Loop formation. Am J Hum Genet. 2018;102(5):776–93.

42. Zhu DL, Chen XF, Hu WX, Dong SS, Lu BJ, Rong Y, Chen YX, Chen H, Thynn HN, Wang NN, et al. Multiple functional variants at 13q14 risk locus for osteoporosis regulate RANKL expression through Long-Range Super-enhancer. J Bone Min Res. 2018;33(7):1335–46.

43. Cho HW, Jin HS, Eom YB. MYLK and PTGS1 Genetic variations Associated with osteoporosis and benign breast tumors in Korean Women. Genes (Basel) 2021, 12(3).

44. Korotkova M, Jakobsson PJ. Persisting eicosanoid pathways in rheumatic diseases. Nat Rev Rheumatol. 2014;10(4):229–41.

45. Wang Y, Liu Y, Zhang M, Lv L, Zhang X, Zhang P, Zhou Y. Inhibition of PTGS1 promotes osteogenic differentiation of adipose-derived stem cells by suppressing NF-kB signaling. Stem Cell Res Ther. 2019;10(1):57.

46. Zhao L. Mitochondrial DNA degradation: a quality control measure for mitochondrial genome maintenance and stress response. Enzymes. 2019;45:311–41.

47. Collins LV, Hajizadeh S, Holme E, Jonsson IM, Tarkowski A. Endogenously oxidized mitochondrial DNA induces in vivo and in vitro inflammatory responses. J Leukoc Biol. 2004;75(6):995–1000.

48. Du J, Yu S, Wang D, Chen S, Chen S, Zheng Y, Wang N, Chen S, Li J, Shen B. Germline and somatic mtDNA mutation spectrum of rheumatoid arthritis patients in the Taizhou area, China. Rheumatology (Oxford). 2020;59(10):2982–91.

49. Gao X, Jiang Z, Yan X, Liu J, Li F, Liu P, Li J, Wei Y, Sun YE, Zhang Y, et al. ATF5, a putative therapeutic target for the mitochondrial DNA 3243A > G mutation-related disease. Cell Death Dis. 2021;12(7):701.

50. Miyazaki T, Iwasawa M, Nakashima T, Mori S, Shigemoto K, Nakamura H, Katagiri H, Takayanagi H, Tanaka S. Intracellular and extracellular ATP coordinately regulate the inverse correlation between osteoclast survival and bone resorption. J Biol Chem. 2012;287(45):37808–23.

Publisher's Note